

The ${}^9\text{Be}({}^8\text{Li}, {}^9\text{Be}){}^8\text{Li}$ elastic-transfer reaction

O. Camargo, V. Guimarães, R. Lichtenthäler, and V. Scarduelli

Instituto de Física, Universidade de São Paulo, P. O. Box 66318, 05389-970 São Paulo, SP, Brazil

J. J. Kolata

Department of Physics, University of Notre Dame, Notre Dame, Indiana 46556, USA

C. A. Bertulani

Department of Physics, Texas A&M University, Commerce, Texas 75429, USA

H. Amro, F. D. Becchetti, and Hao Jiang

Department of Physics, University of Michigan, Ann Arbor, Michigan 48109-1120, USA

E. F. Aguilera, D. Lizcano, E. Martinez-Quiroz, and H. Garcia

Instituto Nacional de Investigaciones Nucleares, A. P. 18-1027, C. P. 11801, Distrito Federal, Mexico

(Received 2 April 2008; revised manuscript received 23 July 2008; published 16 September 2008)

Angular distributions for the ${}^9\text{Be}({}^8\text{Li}, {}^9\text{Be}){}^8\text{Li}$ elastic-transfer reaction have been measured with a 27-MeV ${}^8\text{Li}$ radioactive nuclear beam. Spectroscopic factors for the $({}^9\text{Be}|{}^8\text{Li} + p)$ bound system were obtained from the comparison between the experimental differential cross sections and finite-range distorted-wave Born approximation calculations made with the code FRESKO. The spectroscopic factors so obtained are compared with shell-model calculations and other experimental values. Using the present value for the spectroscopic factors, cross sections and reaction rates for the ${}^8\text{Li}(p, \gamma){}^9\text{Be}$ direct proton-capture reaction of astrophysical interest were calculated in the framework of the potential model.

DOI: [10.1103/PhysRevC.78.034605](https://doi.org/10.1103/PhysRevC.78.034605)

PACS number(s): 21.10.Jx, 25.60.Je, 25.40.Lw

I. INTRODUCTION

Direct reactions, such as one-nucleon transfer reactions, are powerful tools for nuclear structure investigation. The relative simplicity of the reaction mechanism, which usually involves only a few degrees of freedom, allows extraction of experimental structure information as spectroscopic factors or reduced widths. Nowadays, with the improvement of radioactive ion beam intensities, it also is possible to obtain reliable measurements of transfer cross sections induced by unstable projectiles. Recently, we have reported on the measurement and analysis of angular distributions for two neutron-transfer reactions induced by a ${}^8\text{Li}$ radioactive ion beam on a ${}^9\text{Be}$ target [1]: ${}^9\text{Be}({}^8\text{Li}, {}^9\text{Li}){}^8\text{Be}$ and ${}^9\text{Be}({}^8\text{Li}, {}^7\text{Li}){}^{10}\text{Be}$. From finite-range distorted-wave Born approximation (FR-DWBA) analysis of these angular distributions, the spectroscopic factors for the $({}^8\text{Li}_{\text{gs}}|{}^7\text{Li}_{\text{gs}} + n)$ and $({}^9\text{Li}_{\text{gs}}|{}^8\text{Li}_{\text{gs}} + n)$ bound systems were extracted, indicating that these reactions are good and reliable tools to obtain spectroscopic information on these light nuclei. Here we present the result of an analysis of the angular distribution for the ${}^9\text{Be}({}^8\text{Li}, {}^9\text{Be}){}^8\text{Li}$ elastic-transfer reaction. Transfer reactions generally have two vertices, and the spectroscopic factor for one of them has to be known to obtain the spectroscopic factor for the other vertex. The elastic-transfer process, where the elastic scattering and the transfer reaction produce the same exit channel, have the advantage of only one unknown vertex.

Spectroscopic studies of mass $A = 9$ nuclei have been revived recently not only due to applications in nuclear

astrophysics, where spectroscopic factors have been used to obtain capture-reaction cross sections [1,2], but also as important experimental probes for single-particle dynamics. Spectroscopic factors of light nuclei can provide good tests for modern shell-model calculations [3–5]. Here we use the ${}^9\text{Be}({}^8\text{Li}, {}^9\text{Be}){}^8\text{Li}$ elastic-transfer reaction to study proton wave functions in the ground state of ${}^9\text{Be}$. Also, the spectroscopic factor of the $({}^9\text{Be}_{\text{gs}}|{}^8\text{Li}_{\text{gs}} + p)$ bound state, obtained from the present analysis, can be used to determine the nonresonant part of the ${}^8\text{Li}(p, \gamma){}^9\text{Be}_{\text{gs}}$ capture reaction. This capture reaction has some importance in the inhomogeneous Big Bang nucleosynthesis models, where reactions with ${}^8\text{Li}$ can bridge the $A = 8$ mass gap and heavier elements would then be synthesized in the early universe [6]. In this case, not only the ${}^8\text{Li}(n, \gamma){}^9\text{Li}$, ${}^8\text{Li}(\alpha, n){}^{11}\text{B}$, and ${}^8\text{Li}(p, \alpha){}^5\text{He}$ reactions, but also the ${}^8\text{Li}(p, \gamma){}^9\text{Be}$ capture reaction would play important roles in the destruction of ${}^8\text{Li}$ and synthesis of heavier elements. Likewise, in extended network reaction calculations of the r process, light neutron-rich nuclei such as ${}^8\text{Li}$ have been found to be important to produce seed nuclei for this process in type II supernovae [7,8], and the ${}^8\text{Li}(p, \gamma){}^9\text{Be}$ capture reaction has been included. This capture reaction has recently been investigated by using the indirect ANC (asymptotic normalization coefficient) method [9,10], where the ANC coefficient was determined from the ${}^8\text{Li}(d, n){}^9\text{Be}_{\text{gs}}$ reaction in inverse kinematics. Here, we use the potential model framework to determine the ${}^8\text{Li}(p, \gamma){}^9\text{Be}$ capture reaction.

II. THE EXPERIMENT

We have measured the angular distributions for elastic scattering and the ${}^9\text{Be}({}^8\text{Li}, {}^9\text{Be}){}^8\text{Li}$ proton transfer reaction using a 27-MeV ${}^8\text{Li}$ radioactive ion beam on a ${}^9\text{Be}$ target. The details of this experiment have been previously reported elsewhere [1]. Here, only some relevant aspects specific for this measurement are discussed. The ${}^8\text{Li}$ beam was obtained from the *TwinSol* radioactive nuclear beam (RNB) system at the Nuclear Structure Laboratory of the University of Notre Dame, USA [11]. In this system, the secondary ${}^8\text{Li}$ beam is selected in flight by two solenoids that act as magnetic lenses to separate the reaction products from a primary ${}^7\text{Li}$ beam (30 MeV, $1\text{ e}\mu\text{A}$) incident on a 12- μm -thick ${}^9\text{Be}$ target. The two solenoids focused the ${}^8\text{Li}$ secondary beam onto a 1.80-mg/cm²-thick ${}^9\text{Be}$ target. At this point, the ${}^8\text{Li}$ beam had an average intensity of about 5.0×10^5 particles per second per $1\text{ e}\mu\text{A}$ of primary beam. The energy of the ${}^8\text{Li}$ beam at the center of the secondary ${}^9\text{Be}$ target was 27 MeV, and the energy spread was 0.450 MeV (FWHM) determined from an elastic scattering measurement on a gold target. Some secondary beam contaminants, such as ${}^4\text{He}$, ${}^6\text{He}$, ${}^7\text{Li}$, and ${}^9\text{Be}$, which had the same magnetic rigidity as ${}^8\text{Li}$, were also present. The light ${}^4\text{He}$, ${}^6\text{He}$, and ${}^7\text{Li}$ contaminants did not produce reaction products with mass $A = 8$ or $A = 9$ in the same range of energy as the particles from the elastic or transfer reaction of interest. However, ${}^9\text{Be}$ particles coming from the production target as a beam contaminant could also be scattered by the secondary ${}^9\text{Be}$ target and produce ${}^9\text{Be}$ particles with energy very close to, but lower than, those from the transfer reaction.

The scattered ${}^8\text{Li}$ particles and the ${}^9\text{Be}$ reaction products were detected by an array of ΔE - E Si telescopes as described in Ref. [1]. Because the angular aperture of the collimator in front of the detectors spanned about $\pm 3^\circ$, the average detection angles were determined from a Monte Carlo simulation that took into account the collimator size in front of the detectors, the beam spot size on the secondary target (about 4 mm in diameter), the secondary beam divergence, and the angular distribution across the detector aperture. The latter was assumed to be Rutherford for the gold target but was calculated in an iterative way for the ${}^9\text{Be}$ target. The simultaneous measurement of the transfer products and the elastic scattering was very useful to check the consistency of the overall normalization and to select an optimal set of optical-model potential parameters. This was very important in carrying out the FR-DWBA calculations of the transfer reaction. The elastic scattering of ${}^8\text{Li}$ on the gold target (assumed to be Rutherford) was measured to obtain the absolute normalization of the data.

To better identify the reaction products, a two-dimensional $[C(Z, M) \times E_{\text{total}}]$ identification spectrum was constructed using the ΔE and E information from the telescopes. The particle identification constant, $C(Z, M)$, is given by: $C(Z, M) = (E_{\text{total}})^b - (E_{\text{total}} - \Delta E)^b$ [12], where $E_{\text{total}} = \Delta E + E_{\text{residual}}$ and $b = 1.70$ for these light particles. In this spectrum, each $[Z, M]$ particle group appears as an approximately straight line as a function of the particle energy. A typical particle identification spectrum is shown in Fig. 1. As one can see in this figure, the ${}^8\text{Li}$ and ${}^9\text{Be}$ particle groups could easily be resolved.

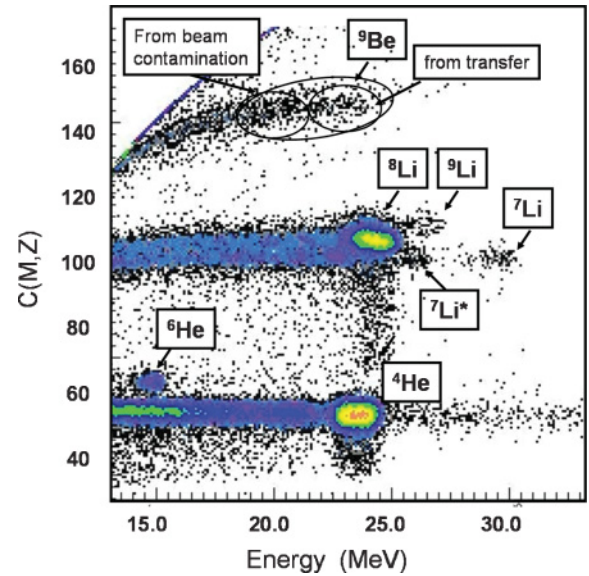


FIG. 1. (Color online) Typical particle identification spectrum $[C(Z, M) \times E_{\text{total}}]$ showing the reaction products from the interaction of ${}^8\text{Li} + {}^9\text{Be}$ at 15° (laboratory). The elastic scattering (${}^8\text{Li}$) and reaction products (${}^7\text{Li}$, ${}^9\text{Li}$, and ${}^9\text{Be}$) are indicated, as well as the ${}^4\text{He}$, ${}^6\text{He}$, and ${}^9\text{Be}$ contamination in the secondary beam.

A. Angular distribution for the ${}^9\text{Be}({}^8\text{Li}, {}^9\text{Be}){}^8\text{Li}$ reaction

The ${}^9\text{Be}$ group indicated in Fig. 1 includes particles coming from the elastic scattering of the ${}^9\text{Be}$ secondary beam contamination on the ${}^9\text{Be}$ target, as well as ${}^9\text{Be}$ from the ${}^9\text{Be}({}^8\text{Li}, {}^9\text{Be}){}^8\text{Li}$ transfer reaction. The projection onto the energy axis of the ${}^9\text{Be}$ group identified in Fig. 1 (which was obtained at 15° laboratory) is presented in Fig. 2. As one can see, the overall experimental energy resolution (0.450 MeV) was sufficient to separate the two groups of ${}^9\text{Be}$ particles. To

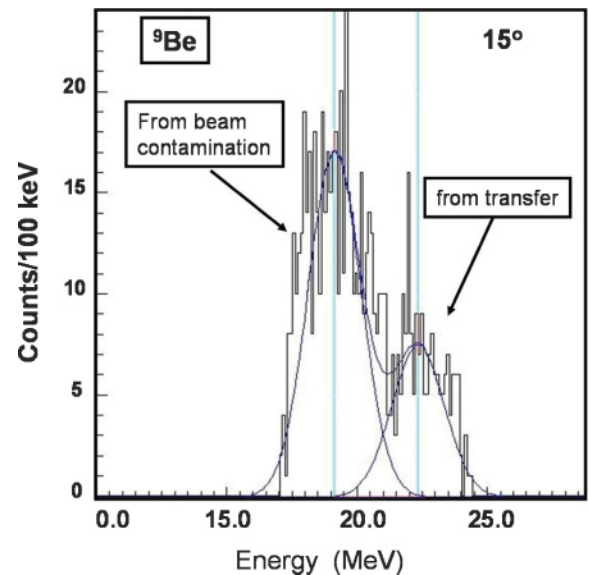


FIG. 2. (Color online) The energy projection from the $C(M, Z) \times \text{Energy}$ plot of the ${}^9\text{Be}$ group, where the two contributions are indicated.

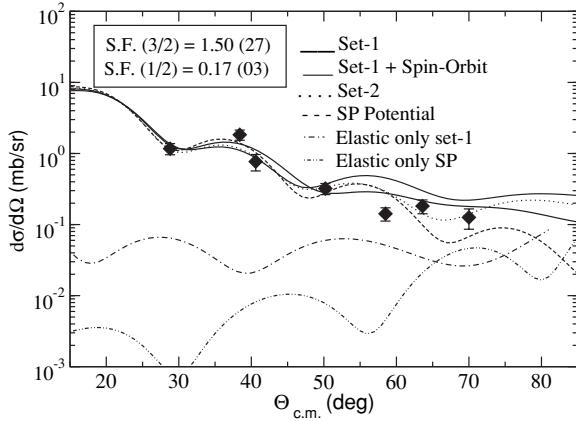


FIG. 3. The differential cross sections for the ${}^9\text{Be}({}^8\text{Li}, {}^9\text{Be}_{\text{gs}}){}^8\text{Li}_{\text{gs}}$ proton transfer reaction at 27 MeV (laboratory) incident energy. The curves are FR-DWBA calculations using the code FRESKO with the potentials indicated (see Table I). The curves are smeared out considering the $\Delta\Theta = 10^\circ$ (in the center of mass) angular aperture of the detectors.

obtain the transfer-reaction yield, a line-shape analysis using Gaussian forms for the peaks was considered for the spectra obtained at forward angles. For the most backward-angle measurements, the ${}^9\text{Be}$ yields were determined based on the expected energy of the group.

The experimental angular distribution obtained for the ${}^9\text{Be}({}^8\text{Li}, {}^9\text{Be}){}^8\text{Li}$ transfer reaction is shown in Fig. 3. The differential cross sections for this transfer process are not very large (in the range of 0.1 to 2 mb/sr), which made the measurements and analysis difficult at the backward angles due to the limited secondary beam intensity. The uncertainties in the differential cross sections were estimated considering the statistical uncertainty in the yields and the systematic uncertainties in the target thickness (10%) and the secondary beam intensity (10%).

In the elastic-transfer process, the entrance and exit channel are the same. Thus, for each angle we would have contributions from both processes, elastic and transfer. These two processes cannot be experimentally distinguished. However, the elastic scattering process is predominant at forward angles and the transfer process predominates at backward angles. The analysis of the ${}^9\text{Be}({}^8\text{Li}, {}^8\text{Li}){}^9\text{Be}$ elastic scattering is described in a previous article [1], where optical-model potential parameters for the ${}^8\text{Li} + {}^9\text{Be}$ system were obtained. In this elastic-scattering analysis, we also considered a double-folding potential, the Sao Paulo potential (SP potential), which is energy dependent and has a nonlocality correction [13] but no free parameters. The sets of potentials considered in

the analysis, including the double-folding potential, all gave a good description of the elastic-scattering data that builds confidence in the experimental absolute normalization.

Analysis of the angular distribution for the ${}^9\text{Be}({}^8\text{Li}, {}^9\text{Be})$ proton transfer reaction was performed using the finite-range distorted-wave Born approximation (FR-DWBA) with the code FRESKO [14]. The results of the FR-DWBA calculations for the transfer reaction can be seen in Fig. 3. Two parameter sets used for both the entrance and exit channels of the DWBA calculations are listed in Table I, indicated as Set-1 and Set-2. The potential parameters indicated as Set-3 were used as the remnant potential for the ${}^8\text{Li}-{}^8\text{Li}$ core-core interaction, where a spin-orbit potential with parameters $V_{\text{SO}} = 2.5$ MeV, $r_{\text{SO}} = 0.950$ fm, and $a_{\text{SO}} = 0.45$ fm was also added. The potential for the bound-state overlap function of the $\langle {}^9\text{Be}_{\text{gs}} | {}^8\text{Li}_{\text{gs}} + p \rangle$ system was taken to be a volume-type Woods-Saxon potential with geometric parameters $r_0 = 1.25$ fm and $a = 0.65$ fm. The depth of the potential, $V_0 = 76.72$ MeV, was obtained by adjusting it to reproduce the proton binding energy (BE = 16.888 MeV). In the present FR-DWBA calculation, the proton from the ${}^9\text{Be}({}^8\text{Li}, {}^9\text{Be}_{\text{gs}}){}^8\text{Li}_{\text{gs}}$ pickup reaction is assumed to be transferred to either the $1p_{1/2}$ or $1p_{3/2}$ orbits in the ${}^9\text{Be}$ ground state ($J^\pi = 3/2^-$). In this case, the spectroscopic factor for the $\langle {}^9\text{Be}_{\text{gs}} | {}^8\text{Li}_{\text{gs}} + p \rangle$ vertex has two contributions, corresponding to protons in the $p_{3/2}$ and $p_{1/2}$ orbital in ${}^9\text{Be}_{\text{gs}}$. FR-DWBA calculations with these two contributions gave angular distributions that were very similar in shape and differed only in absolute value. We therefore could not distinguish them in the present analysis and instead constrained the spectroscopic factor of the $p_{1/2}$ orbital to be 11% of that for the $p_{3/2}$ state, based on the calculations of Cohen and Kurath [15]. The results of FR-DWBA calculations considering a coherent sum of these two contributions are shown in Fig. 3 for various sets of parameters. As one can see, the calculations agree relatively well with the data at forward angles to within experimental uncertainties.

The spectroscopic factors were obtained by normalizing the calculated cross section to the data, considering the ratio of 11% for the $p_{1/2}$ and $p_{3/2}$ orbital and taking into account the cross sections at the three most-forward angles. The pure elastic scattering contribution in this angular region was estimated with the code FRESKO and is shown in Fig. 3. At forward angles, the elastic scattering contribution is calculated to be very small (less than 5% for the optical potential Set-1 and less than 1% for the double folding SP potential). This contribution is then added in quadrature to the uncertainty in the spectroscopic factor.

Calculations for the transfer reaction made with the various parameter sets (Set-1, Set-2, and double-folding potential) for

TABLE I. Optical-model potential parameters. Radii are given by $R_x = r_x \times A_T^{1/3}$. The real and imaginary potentials are volume type Woods-Saxon. The depths are in MeV and the radius and diffuseness are in fm.

Set	V	r_R	a_R	W_V	r_I	a_I	r_C	References
1	173.1	1.19	0.78	8.90	2.52	0.924	1.78	${}^7\text{Li} + {}^9\text{Be}$ at 34 MeV [16]
2	234.4	1.21	0.76	8.90	2.43	1.020	1.78	${}^7\text{Li} + {}^9\text{Be}$ at 34 MeV [16]
3	107.8	0.750	0.855	37.9	0.910	0.757	1.4	${}^7\text{Li} + {}^7\text{Li}$ at 42 MeV [17]

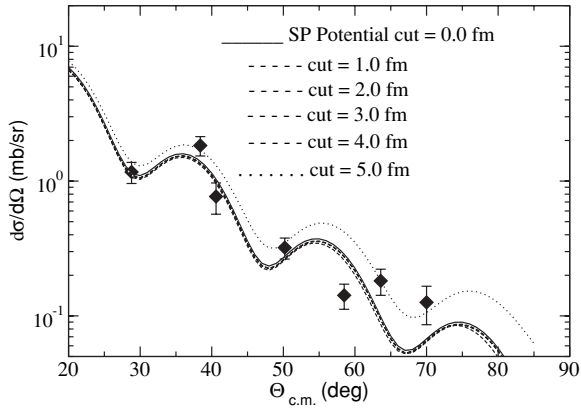


FIG. 4. Angular distribution for the ${}^9\text{Be}({}^8\text{Li}, {}^9\text{Be}_{\text{gs}}){}^8\text{Li}_{\text{gs}}$ proton transfer reaction at 27 MeV incident energy. The solid line corresponds to the FR-DWBA calculation with the double-folding SP potential (Sao Paulo potential). The dashed lines are FR-DWBA calculations with cutoffs in the radial form factor integral as indicated. The calculated curves are smeared out as in Fig. 3.

the entrance and exit channels gave slightly different values for the spectroscopic factors. The adopted values of the spectroscopic factors for the two contributions, $({}^9\text{Be}_{\text{gs}}(1/2)|{}^8\text{Li}_{\text{gs}} + p)$ and $({}^9\text{Be}_{\text{gs}}(3/2)|{}^8\text{Li}_{\text{gs}} + p)$, are taken as the average value of the three determinations. The uncertainties are due to the uncertainty in the experimental data at forward angles (15%) and the dispersion of the values obtained with the different parameter sets (11%). (It should be noted that these values are based also on the assumed 11% $p_{1/2} / p_{3/2}$ ratio.) The results are compared with other experimental values and shell-model calculations in Table II. Our results agree very well within experimental error with the values from the shell-model calculation of Ref. [15] but are much higher than the experimental value obtained from a recent ${}^8\text{Li}(d, n){}^9\text{Be}$ reaction [9]. A similar situation, where the spectroscopic factor for both vertices involved in the transfer reaction agree with values calculated by Cohen and Kurath, has been found in the analysis of the ${}^9\text{Be}({}^8\text{Li}, {}^7\text{Li}){}^{10}\text{Be}$, ${}^9\text{Be}({}^8\text{Li}, {}^9\text{Li}){}^8\text{Be}$ [1], ${}^9\text{Be}({}^7\text{Li}, {}^6\text{Li}){}^{10}\text{Be}$ [16], and ${}^9\text{Be}({}^6\text{Li}, {}^7\text{Li}){}^8\text{Be}$ [19] neutron transfer reactions. These results indicate that Cohen-Kurath wave functions describe lithium and beryllium isotopes in the mass range $A = 6$ to $A = 10$ reasonably well.

The peripherality of a transfer reaction can be verified by testing the influence of the internal part of the overlap function

on the angular distribution. This can be done by increasing the lower radius cutoff in the radial FR-DWBA integrals from zero up to the radius corresponding to the closest approach of the two interacting nuclei, $R_{\text{cut}} = 1.25(A_p^{1/3} + A_t^{1/3}) = 5.1$ fm. We performed such a test for the ${}^9\text{Be}({}^8\text{Li}, {}^9\text{Be}){}^8\text{Li}$ transfer reaction and the results of FR-DWBA calculations using the SP potential are presented in Fig. 4. As one can see, the radius cutoff produced no change in the calculation in the angular range from 0° to 90° for a radius cut $R_{\text{cut}} < 5.0$ fm. Thus, we conclude that this transfer reaction is indeed peripheral at the energy and angles considered here.

B. Astrophysical S factor for the ${}^8\text{Li}(p, \gamma){}^9\text{Be}$ capture reaction

The direct radiative capture (DRC) of an s - and/or d -wave proton by a nucleus b , proceeding by an $E1$ transition and leaving the compound nucleus c in its ground state, is given by:

$$\sigma_{b \rightarrow c}^{E1}(p, \gamma) = \frac{16\pi}{9\hbar} k_\gamma^3 |\langle \psi_{\text{scat}} | O^{E1} | I_{\text{bound}} \rangle|^2, \quad (1)$$

where $k_\gamma = \epsilon_\gamma / \hbar c$ is the wave number corresponding to a γ -ray energy ϵ_γ , O^{E1} stands for the electric dipole operator, and the initial-state wave function ψ_{scat} is the incoming nucleon wave function scattered by the nucleon-nucleus potential. Usually, in astrophysics, we use the astrophysical S factor, which is related to the cross section of the capture reaction by the expression: $S(E) = E \sigma_{\text{cap}}(E) \exp(2\pi\eta)$, where η is the Sommerfeld parameter.

The essential ingredients in these calculations are the potentials used to generate the wave functions ψ_{scat} and I_{bound} , and the normalization for the latter that is given by its spectroscopic factor or, alternatively, by the reduced width or ANC when the capture is peripheral. For a peripheral capture reaction, the overlap function I_{bound} of the single particle bound state can be determined by either considering the spectroscopic factor or reduced width or the ANC. The two latter methods have less sensitivity to the choice of the bound-state potential parameters. Also, for a peripheral capture reaction, the ψ_{scat} wave function, which describes the particles in the continuum, can be determined by just considering the Coulomb wave function. However, due to the tight binding of the last proton in ${}^9\text{Be}$ ($\text{BE} = 16.888$ MeV), the contribution of the internal part of the interaction potential for the ${}^8\text{Li} + p$ system is important

TABLE II. Spectroscopic factors C^2S .

	Shell-model calculation	(d, n)	$(d, {}^3\text{He})$	This work
${}^8\text{Li}_{\text{gs}} \otimes p = {}^9\text{Be}_{\text{gs}}(p_{3/2})(J^\pi = 3/2^-)$	1.356 ^a	0.64 ^b	1.50 ^c	1.50 (28) ^d
${}^8\text{Li}_{\text{gs}} \otimes p = {}^9\text{Be}_{\text{gs}}(p_{1/2})(J^\pi = 3/2^-)$	0.153 ^a			0.17 (03) ^e

^aFrom Cohen and Kurath [15].

^bFrom the $d({}^8\text{Li}, n){}^9\text{Be}$ reaction at 40 MeV [9].

^cFrom the ${}^9\text{Be}(d, {}^3\text{He}){}^8\text{Li}$ reaction at 52 MeV [18].

^dAverage of 1.435, 1.638, 1.440 from Set 1, Set 2, and SP potentials.

^eAverage of 0.158, 0.183, 0.158 from Set 1, Set 2, and SP potentials.

and the nuclear part of the interaction plays an important role in the capture reaction. Thus, to calculate the cross section for the direct capture reaction ${}^8\text{Li}(p, \gamma){}^9\text{Be}$, we consider here the framework of the potential model [20]. To perform this calculation in this framework we used the computer code RADCAP [21].

In the low-energy region of astrophysical relevance, the ${}^8\text{Li}(p, \gamma){}^9\text{Be}$ capture reaction proceeds by the $E1$ radiative capture of an s -wave (and also d -wave for energies above 1.0 MeV) proton. In the potential model framework, the potentials generate the ψ_{scat} wave function and the I_{bound} overlap function, where the latter has to be normalized by the corresponding spectroscopic factor. The overlap function, I_{bound} , of the ${}^9\text{Be}_{\text{gs}}(J^\pi = 3/2^-)|{}^8\text{Li} + p\rangle$ bound state, has been determined using a volume Woods-Saxon potential type having geometric parameters $R = r_0 \times A_T^{1/3}$ fm with $r_0 = 1.25$ and $a = 0.65$ fm. The depth $V_0 = 76.72$ MeV for this potential was obtained to reproduce the binding energy of the proton in ${}^9\text{Be}$. The spectroscopic factor for the bound system was obtained from the analysis of the ${}^9\text{Be}({}^8\text{Li}, {}^9\text{Be}_{\text{gs}}){}^8\text{Li}_{\text{gs}}$ elastic-transfer reaction described in the previous section. The potential parameters necessary to generate the ψ_{scat} wave function for the ${}^8\text{Li} + p$ scattering system can also be determined assuming a Woods-Saxon volume potential with geometric parameters $r_0 = 1.25$ and $a = 0.65$ fm. The depth V_0 for this potential is usually obtained from the scattering length of the nucleon-nucleus system. However, because no experimental value for the scattering length of the $p + {}^8\text{Li}$ system is available, an indirect method has to be used to obtain the corresponding depth of the scattering potential.

In most works based on the idea of the ANC, the capture reaction at stellar energies is assumed to proceed through the tail of the nuclear overlap function, and thus the amplitude of the radiative capture cross section is dominated by contributions from large relative distances of the participating nuclei. In this case, the $S \times I_{\text{bound}}$ product, where S is the spectroscopic factor, can be written in the asymptotic form as: $\text{ANC} \times W_{-\eta, l+1/2}(2\kappa r)$. Here $W_{-\eta, l+1/2}(2\kappa r)$ is the Whittaker function and ψ_{scat} is assumed to be due only to the Coulomb potential. However, in general, capture reactions of light nuclei are not necessarily peripheral and the nuclear potential of the interacting nuclei can play an important role. To show the importance of the scattering potential depth V_0 on the capture cross section, we calculated the astrophysical S factor, $S(E, V_0)$, at $E = 0$, $S(0, V_0)$ as a function of V_0 , scaled to the S factor calculated with a pure Coulomb wave function $S(0, 0)$, for both the ${}^8\text{B} + p$, ${}^6\text{Li} + p$, and ${}^8\text{Li} + p$ systems. These systems are close in mass but have very different proton binding energies ($\text{BE} = 1.296$ MeV for ${}^8\text{B} + p$, $\text{BE} = 5.606$ MeV for ${}^6\text{Li} + p$ and $\text{BE} = 16.888$ MeV for ${}^8\text{Li} + p$). The results of these calculations, also using the computer code RADCAP [21], are presented in Fig. 5. A similar analysis has been performed before by Typel and Baur for other proton capture reactions, including also the ${}^8\text{B} + p$ system [22]. The important feature of these calculations is to demonstrate the sensitivity of the astrophysical S factor to the choice of the scattering potential depth V_0 and to emphasize the appearance of resonances in the potential. As one can see in Fig. 5, the S factor for both ${}^8\text{Li} + p$ and ${}^8\text{B} + p$ shows resonant

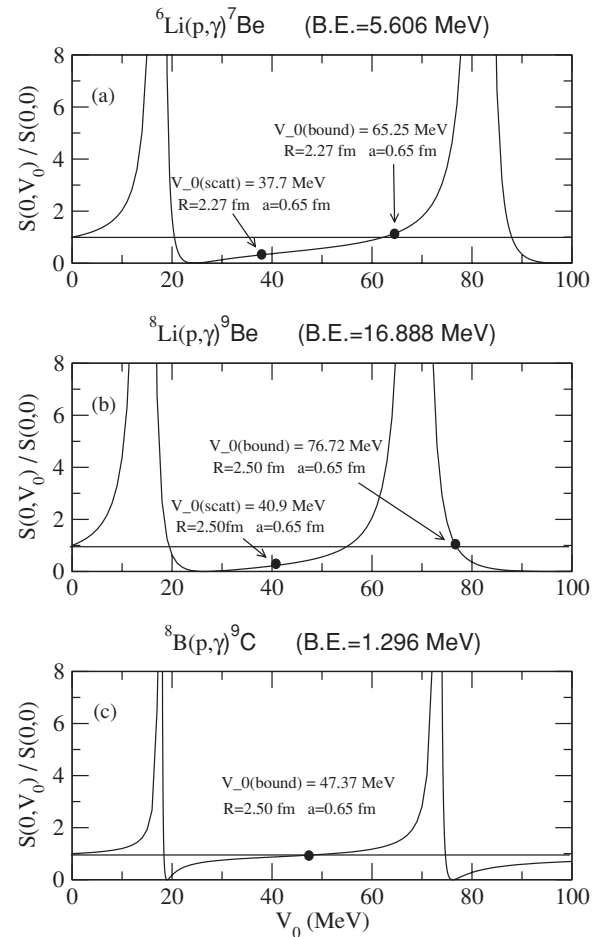


FIG. 5. S factor at $E = 0$ as a function of scattering potential depth V_0 , $S(E, V_0)$, scaled to the S factor calculated with a pure Coulomb wave function, $S(0, V_0)/S(0, 0)$, for the ${}^6\text{Li} + p$, ${}^8\text{Li} + p$, and ${}^8\text{B} + p$ systems. The depths $V_0(\text{scatt})$ and $V_0(\text{bound})$ used in the calculations are indicated for each system.

behavior for specific values of V_0 of the continuum potential. It is also clear in the figure that the sensitivity to the depth of the potential is higher for the more tightly bound system, ${}^8\text{Li} + p$, as compared with the ${}^8\text{B} + p$ system. The resonances shown in Fig. 5 are quasibound states in the potential used to describe the ${}^8\text{Li} + p$ system in the continuum.

To calculate the cross section and subsequent astrophysical S factor for the direct (nonresonant) capture reaction ${}^8\text{Li}(p, \gamma){}^9\text{Be}$ of the potential model, we therefore need to consider a model for the potentials used to describe the continuum and bound $p + {}^8\text{Li}$ system. Here we adopted a volume Woods-Saxon shape for both potentials. Mengoni *et al.* [23] have suggested using the same potential for both the incoming scattering channel and the bound state in the cross-section calculation. As indicated in Fig. 5, this choice of scattering potential gives an astrophysical S factor very close to that for $V_0 = 0$ (pure Coulomb scattering). We adopt a scattering potential depth that gives the same volume integral of the optical potential, $J_V/A = 558 \pm 25$ MeV \times fm/nucleon, as that obtained from the analysis of the ${}^6\text{Li}(p, \gamma){}^7\text{Be}_{\text{gs}}$ capture reaction. The volume integral

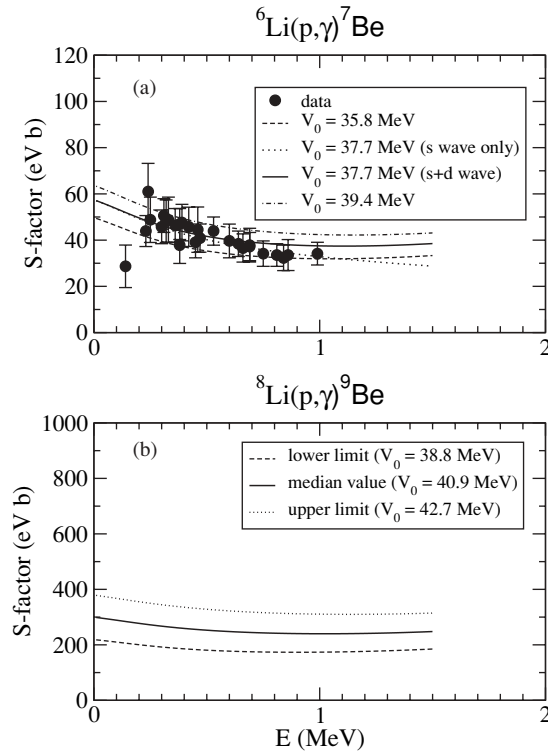


FIG. 6. The astrophysical S factor for the direct capture reaction of an s and d proton wave: (a) for the ${}^6\text{Li}(p, \gamma){}^7\text{Be}_{\text{gs}}$ capture reaction (the experimental points are from Ref. [25]); (b) for ${}^8\text{Li}(p, \gamma){}^9\text{Be}$. The values of the scattering potential depth V_0 for the upper and lower limits are indicated.

is a reliable alternative method to obtain this potential depth because it is known to vary less strongly for different systems than the potential parameters themselves [24].

The known experimental values of the capture cross sections for the ${}^6\text{Li}(p, \gamma){}^7\text{Be}_{\text{gs}}$ capture reaction were obtained by multiplying the total cross sections from Ref. [25] by a factor of 0.61. This factor corresponds to the ${}^7\text{Be}$ ground-state branch of 61% of the total (p, γ) reaction as quoted also in Ref. [25]. The experimental astrophysical $S(E_{\text{c.m.}})$ factor for each of the measured energies is obtained using the expression from Ref. [30]:

$$S(E_{\text{c.m.}}) = \sigma(E_{\text{c.m.}}) \times E_{\text{c.m.}} \times \exp(+2\pi\eta), \quad (2)$$

where $\eta = 0.1575 \times Z_1 Z_2 \times (\mu/E_{\text{c.m.}})^{1/2}$ is the Sommerfeld parameter, $E_{\text{c.m.}}$ is the relative energy in the center of mass, Z_1 and Z_2 are the atomic numbers for the projectile (p) and target (${}^6\text{Li}$), respectively, and μ is the reduced mass.

The obtained experimental $S(E_{\text{c.m.}})$ values for the ${}^6\text{Li} + p$ system are presented in Fig. 6(a). To calculate the astrophysical S factor for this system we used the potential model described above, with s - and d -wave proton capture given by an $E1$ transition from the ${}^6\text{Li}(J^\pi = 1^+)$ nucleus to form ${}^7\text{Be}(J^\pi = 3/2^-)$. The spectroscopic factor for the $({}^7\text{Be}_{\text{gs}}(3/2^-)|{}^6\text{Li}_{\text{gs}}(1^+) + p|)$ bound system, $S_{7\text{Be}}(\text{gs}, 3/2) = 0.83 \pm 0.09$, was obtained by averaging the

experimental values from the ${}^6\text{Li}(d, p){}^7\text{Li}$ and ${}^7\text{Li}(p, d){}^6\text{Li}$ reactions [27–29]. The bound state and the scattering potential were again taken to be volume Woods-Saxon potentials with geometric parameters $r_0 = 1.25$ and $a = 0.65$ fm. The bound-state potential depth $V_0(\text{bound}) = 65.25$ MeV was obtained by reproducing the binding energy ($\text{BE} = 5.606$ MeV) of the ${}^6\text{Li} + p$ system. The scattering potential depth $V_0(\text{scat}) = 37.7^{+1.7}_{-1.9}$ MeV was determined by adjusting the calculated S factor to reproduce the experimental data of the ${}^6\text{Li}(p, \gamma){}^7\text{Be}$ reaction, as shown in Fig. 6(a). Once we verified that the procedure to obtain the parameters used in the potential model calculation reproduces well the experimentally known cross section for the ${}^6\text{Li}(p, \gamma){}^7\text{Be}_{\text{gs}}$ capture reaction, we extended this procedure to ${}^8\text{Li}(p, \gamma){}^9\text{Be}_{\text{gs}}$.

To calculate the ${}^8\text{Li}(p, \gamma){}^9\text{Be}_{\text{gs}}$ direct capture cross section, we also considered s - and d -wave proton capture via an $E1$ transition to form the ${}^9\text{Be}(J^\pi = 3/2^-)$ compound nucleus. The spectroscopic factors $S_{9\text{Be}}(\text{gs}, 3/2) = 1.50 \pm 0.28$ and $S_{9\text{Be}}(\text{gs}, 1/2) = 0.17 \pm 0.03$ were obtained from the analysis of the ${}^9\text{Be}({}^8\text{Li}, {}^9\text{Be}_{\text{gs}}){}^8\text{Li}_{\text{gs}}$ elastic-transfer reaction. The depth of the bound-state potential was determined to be $V_0(\text{bound}) = 76.72$ MeV to reproduce the binding energy of the ${}^8\text{Li} + p = {}^9\text{Be}$ system. Keeping the same $J_V/A = 558 \pm 25$ MeV \times fm/nucleon as for the ${}^6\text{Li} + p$ system, we determined the depth $V_0(\text{scat}) = 40.9^{+1.8}_{-2.1}$ MeV for the scattering potential of the ${}^8\text{Li} + p$ system. Using these potentials and the spectroscopic factors, the S factor for the nonresonant part of the s -wave and d -wave ${}^8\text{Li}(p, \gamma){}^9\text{Be}_{\text{gs}}$ capture reaction was calculated as a function of relative energy. The results of these calculations are shown in Fig. 6(b). The upper and lower limits are obtained considering the uncertainties in the depth of the scattering potential. The two approaches used to obtain the depth of the potential in the continuum (the use of the same volume integral as for the ${}^6\text{Li} + p$ and the same potential as the bound state) allow a reliable calculation of the direct capture reaction because both values of $V_0(\text{scat})$ lie outside the range of resonances in the potential.

The S factor obtained in this work for the ${}^8\text{Li}(p, \gamma){}^9\text{Be}_{\text{gs}}$ reaction is a factor of 2.6 higher as compared with the value obtained from Ref. [9]. This factor comes from the spectroscopic factors used in the calculations ($\text{SF} = 1.67$ in the present work and 0.64 in Ref. [9]).

There are some speculations in the literature about the fact that absolute spectroscopic factors (SF) obtained from nucleon transfer reactions induced by deuteron or heavier nuclei are model dependent and may be systematically high due to the fact that these reactions probe only the asymptotic region of the overlap integrals. However, a recent extensive survey of neutron spectroscopic factors by Tsang *et al.* [31] indicated a good overall agreement between measured relative SF from (d, p) and (p, d) reactions and large basis shell-model calculations.

Also, in the present work, we have shown that the experimental S factors as a function of energy for the ${}^6\text{Li}(p, \gamma){}^7\text{Be}_{\text{gs}}$ reaction are well-reproduced using the potential model employed here. We therefore assume that the same technique, with similar potential parameters, can be applied to the calculation of the S factors for the ${}^8\text{Li}(p, \gamma){}^9\text{Be}_{\text{gs}}$ reaction.

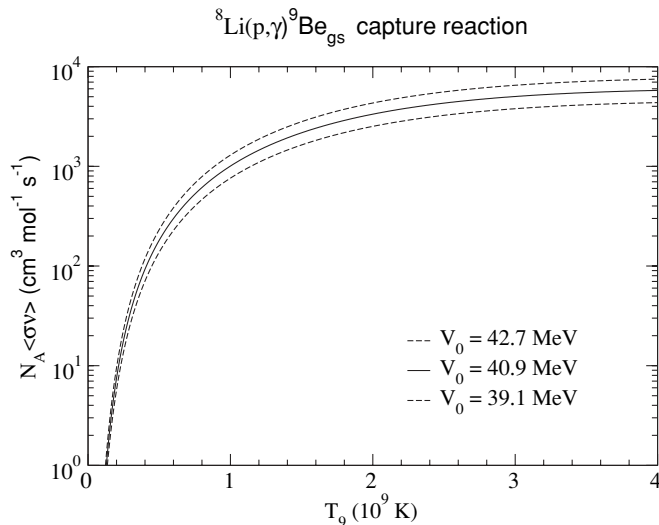


FIG. 7. Reaction rate for the ${}^8\text{Li}(p, \gamma){}^9\text{Be}_{\text{gs}}$ capture reaction as a function of temperature. This reaction rate has been calculated by integrating over the relative energy up to 1.2 MeV.

C. Reaction rate for the ${}^8\text{Li}(p, \gamma){}^9\text{Be}_{\text{gs}}$ capture reaction

We have also computed the nucleosynthesis reaction rate as a function of the temperature for the direct ${}^8\text{Li}(p, \gamma){}^9\text{Be}_{\text{gs}}$ capture reaction. The expression for the reaction rate for $E1$ capture in $\text{cm}^3\text{mol}^{-1}\text{s}^{-1}$ is given by [26]:

$$N_A\langle\sigma v\rangle = K \int_0^\infty \sigma(E)E \exp(-C_2E/T_9) dE, \quad (3)$$

where

$$K = C_1\mu^{-1/2}T_9^{-3/2}$$

and $C_1 = 3.7313 \times 10^{10}$, $C_2 = 11.605$, N_A is Avogadro's number, μ is the reduced mass of the system, T_9 is the temperature in units of 10^9 K, σ is the capture cross section, v is the relative velocity, and E is the energy in the center-of-mass system. E is given in MeV and the cross section in barns. The results of this calculation can be seen in Fig. 7. Although some resonances above the ${}^8\text{Li} + p$ threshold in ${}^9\text{Be}$ could be important, in the present calculation only the direct capture to the ${}^9\text{Be}_{\text{gs}}$ is considered. The reaction rate for the ${}^8\text{Li}(p, \gamma){}^9\text{Be}_{\text{gs}}$ capture reaction at temperature $T_9 = 1$ was deduced to be $N_A\langle\sigma v\rangle = (1.0 \pm 0.3) \times 10^3 \text{ cm}^3\text{mol}^{-1}\text{s}^{-1}$, where the uncertainty is from the uncertainty in the scattering potential depth and in the spectroscopic factor for $\langle{}^9\text{Be}_{\text{gs}}|{}^8\text{Li} + p\rangle$ used in the calculation. This value is about 2.5 times larger than the value obtained in Ref. [9].

As suggested by Mengoni *et al.* [23], a different assumption would be to use the same potential for the incoming channel as that for the bound state. With this assumption for the p - ${}^8\text{Li}$ scattering potential, the reaction rate is determined at $T_9 = 1$ to be $N_A\langle\sigma v\rangle = (2.8 \pm 0.5) \times 10^3 \text{ cm}^3\text{mol}^{-1}\text{s}^{-1}$, where the uncertainty comes from the uncertainty in the spectroscopic factor (18%). These two assumptions for the scattering potential produce different reaction rates at temperature $T_9 = 1$. The choice of scattering potential as the same as for the bound state gives a S factor corresponding to a pure Coulomb interaction, as shown in Fig. 5(b). By its turn, the choice of scattering potential keeping the $J_V/\text{nucleon}$ as for the ${}^6\text{Li} + p$, although it is out of the resonance range, it indicates an influence of the interior part of the ${}^8\text{Li} + p$ potential. This is also the case for the ${}^6\text{Li} + p$ system for which the present procedure reproduced the experimental data.

III. SUMMARY

We have measured the angular distributions for the ${}^9\text{Be}({}^8\text{Li}, {}^9\text{Li}){}^9\text{Be}$ elastic-transfer reaction at a ${}^8\text{Li}$ incident energy of $E_{\text{lab}} = 27.0$ MeV. Spectroscopic factors for the $\langle{}^9\text{Be}_{\text{gs}}|{}^8\text{Li} + p\rangle$ system were obtained from the comparison between the experimental differential cross sections and FRDWBA calculations using the code FRESKO. The spectroscopic factors were compared with Cohen-Kurath shell-model calculations and with experimental values from (d, n) and $(d, {}^3\text{He})$ reactions. Using the spectroscopic factors extracted from the experimental angular distributions of the $\langle{}^9\text{Be}_{\text{gs}}|{}^8\text{Li} + p\rangle$ bound system, we have derived the cross sections for the ${}^8\text{Li}(p, \gamma){}^9\text{Be}$ proton capture reaction based on a potential model. The astrophysical S factor and reaction rate for the nonresonant part of the ${}^8\text{Li}(p, \gamma){}^9\text{Be}_{\text{gs}}$ reaction were compared with the results from previous indirect methods. Our work has shown that low-energy radioactive nuclear beams can be very suitable not only to perform spectroscopic investigations but also to determine the nonresonant parts of capture reactions of astrophysical interest.

ACKNOWLEDGMENTS

The authors from Brazil thank the Fundação de Amparo a Pesquisa do Estado de São Paulo (FAPESP 2001/06676-9 and 2006/00629-2) for financial support. This work was also funded in part by the U.S. NSF under grant nos. PHY03-54828 and INT03-05347. The author C.A.B. was partially supported by the U.S. Department of Energy under contract no. DE-FG02-08ER41533, and DE-FC02-07ER41457 (UNEDF, SciDAC-2). The authors from Mexico thank the partial support by CONACYT.

- [1] V. Guimarães *et al.*, Phys. Rev. C **75**, 054602 (2007).
 [2] Z. H. Li *et al.*, Phys. Rev. C **71**, 052801(R) (2005).
 [3] A. H. Wuosmaa *et al.*, Phys. Rev. Lett. **94**, 082502 (2005).
 [4] P. Navrátil, Phys. Rev. C **70**, 054324 (2004).
 [5] G. V. Rogachev, J. J. Kolata, A. S. Volya, F. D. Becchetti, Y. Chen, P. A. DeYoung, and J. Lupton, Phys. Rev. C **75**, 014603 (2007).

- [6] T. Kajino and R. N. Boyd, Astrophys. J. **359**, 267 (1990).
 [7] M. Terasawa, K. Sumiyoshi, T. Kajino, G. J. Mathews, and I. Tanihata, Astrophys. J. **562**, 470 (2001).
 [8] T. Kajino, S. Wanajo, and G. J. Mathews, Nucl. Phys. A **704**, 165c (2002).

- [9] J. Su, Z. H. Li, B. Guo, W. P. Liu, X. X. Bai, S. Zeng, G. Lian, S. Q. Yan, B. X. Wang, and Y. B. Wang, *Chin. Phys. Lett.* **23**, 55 (2006).
- [10] C. A. Gagliardi, A. Azhari, V. Burjan, F. Carstoiu, V. Kroha, A. M. Mukhamedzhanov, A. Sattarov, X. Tang, L. Trache, and R. E. Tribble, *Eur. Phys. J.* **A13**, 227 (2002).
- [11] F. D. Becchetti *et al.*, *Nucl. Instrum. Methods Phys. Research A* **505**, 377 (2003).
- [12] G. F. Knoll, *Radiation Detection and Measurement* (John Wiley & Sons, New York, 1989), p. 380.
- [13] L. C. Chamon, B. V. Carlson, L. R. Gasques, D. Pereira, C. De Conti, M. A. G. Alvarez, M. S. Hussein, M. A. Cândido Ribeiro, E. S. Rossi, Jr., and C. P. Silva, *Phys. Rev. C* **66**, 014610 (2002).
- [14] I. J. Thompson, *Comput. Phys. Rep.* **7**, 167 (1988) and www.fresco.org.uk.
- [15] S. Cohen and D. Kurath, *Nucl. Phys.* **A101**, 1 (1967).
- [16] K. W. Kemper, G. E. Moore, R. J. Puigh, and R. L. White, *Phys. Rev. C* **15**, 1726 (1977).
- [17] O. A. Momotyuk *et al.*, *Phys. Lett.* **B640**, 13 (2006).
- [18] U. Schwinn, G. Mairle, G. J. Wagner, and Ch. Ramer, *Z. Phys. A* **275**, 241 (1975).
- [19] J. Cook and K. W. Kemper, *Phys. Rev. C* **31**, 1745 (1985).
- [20] K. Langanke, *Nucl. Phys.* **A457**, 351 (1986).
- [21] C. A. Bertulani, *Comput. Phys. Commun.* **156**, 123 (2003).
- [22] S. Typel and G. Baur, *Nucl. Phys.* **A759**, 247–308 (2005).
- [23] A. Mengoni, T. Otsuka, and M. Ishihara, *Phys. Rev. C* **52**, R2334 (1995).
- [24] G. R. Satchler, *Introduction to Nuclear Reactions*, second edition (Oxford University Press, New York, 1990), p. 192.
- [25] Z. E. Switkowski, J. C. P. Heggie, D. L. Kennedy, D. G. Sargood, F. C. Barker, and R. H. Spear, *Nucl. Phys.* **A331**, 50–60 (1979).
- [26] C. Angulo *et al.*, *Nucl. Phys.* **A656**, 3 (1999).
- [27] J. P. Schiffer *et al.* *Phys. Rev.* **164**, 164 (1967).
- [28] I. S. Towner, *Nucl. Phys.* **A126**, 97 (1969).
- [29] B. Fagerstrom, J. Kallne, O. Sundberg, and G. Tibell, *Phys. Scr.* **13**, 101 (1976).
- [30] V. Pandharipande, I. Sick, and P. K. A. deWitt Huberts, *Rev. Mod. Phys.* **69**, 981 (1997).
- [31] M. B. Tsang, J. Lee, and W. G. Lynch, *Phys. Rev. Lett.* **95**, 222501 (2005).